

MOL # 8250

**Cytoplasmic Confinement of Breast Cancer Resistance Protein (BCRP/ABCG2) as a Novel
Mechanism of Adaptation to Short-Term Folate Deprivation**

Ilan Ifergan, Gerrit Jansen and Yehuda G. Assaraf

Department of Biology, Technion-Israel Institute of Technology, Haifa 32000, Israel (I.I.,
Y.G.A) and Department of Rheumatology, VU University Medical Center, De Boelelaan 1117,
1081 HV Amsterdam, the Netherlands (G.J.).

Running Title: Folate deficiency and ER Retention of ABCG2.

Address correspondence to: Dr. Yehuda G. Assaraf, Department of Biology, Technion-Israel
Institute of Technology, Haifa 32000, Israel. E-mail: assaraf@tx.technion.ac.il

The abbreviations used are: BCRP, Breast Cancer Resistance Protein; MRP1, Multidrug Resistance Protein 1; Pgp, P-glycoprotein; FPGS, Folylpoly- γ -glutamate synthetase; EGFR, Epidermal growth factor receptor; FGFR, Fibroblast growth factor receptor; MHC, Major histocompatibility complex ; ER, endoplasmic reticulum; NF, no folate; HF, high folate; PBS, Phosphate-buffered saline; MR, mitoxantrone; DAPI, 4,6-diamidino-2-phenylindole hydrochloride.

Footnote: This study was supported by research grants from the Israel Cancer Association and the Star Foundation (to Y.G.A) and Dutch Cancer Society (NKB 2000-2237, to G.J.).

Abstract: 250 words.

Introduction: 662 words.

Materials and Methods: 1698 words.

Results: 1871 words.

Discussion: 1691 words.

Number of references: 32.

Number of Figures: 10.

Number of pages in the manuscript: 34.

Abstract

The unique capability of breast cancer resistance protein (BCRP/ABCG2) to export mono-, di- and triglutamates of folates should limit cellular proliferation under conditions of folate deprivation, particularly upon BCRP overexpression. Here we explored the mode of adaptation of BCRP-overexpressing cells to short-term folate deprivation. MCF-7/MR cells grown in high folate medium (2.3 μ M folic acid) containing mitoxantrone had 70% of their overexpressed BCRP in the plasma membrane and only 30% in the cytoplasm. In contrast, cells grown for two weeks in folic acid-free medium followed by an adaptation week in low folate medium (1 nM folic acid) had 86% of BCRP in the cytoplasm and only 14% in the plasma membrane. Unlike BCRP, various transmembrane proteins retained their normal plasma membrane localization in folate-deprived cells. Folate deprivation was also associated with a 3-fold decrease in BCRP and multidrug resistance protein 1 (MRP1/ABCC1) levels. Confocal microscopy with folate-deprived cells revealed that cytoplasmic BCRP co-localized with calnexin, an established endoplasmic reticulum resident. Consistently, the loss of BCRP from the plasma membrane in folate-deprived cells resulted in a 4.5-fold increase in [3 H]folic acid accumulation relative to MCF7/MR cells. Hence, cellular adaptation to short-term folate deprivation results in a selective confinement of BCRP to the cytoplasm along with a moderate decrease in BCRP and MRP1 levels aimed at preserving the poor intracellular folate pools. These results constitute a novel mechanism of cellular adaptation to short-term folate deprivation and provide further support to the possible role of BCRP in the maintenance of cellular folate homeostasis.

Introduction

Several members of the large ATP-binding cassette (ABC) superfamily of transport proteins have the facility to translocate an extraordinarily diverse array of structurally distinct endogenous and exogenous substrates and their metabolites across cell membranes (Reviewed in Borst and Elferink, 2002; Haimeur et al., 2004; Sarkadi et al., 2004). Among these are three anticancer drug efflux transporters; the multidrug resistance protein 1 (MRP1/ABCC1) (Cole et al., 2004), breast cancer resistance protein (BCRP/ABCG2) (Doyle et al., 2003; Sarkadi et al., 2004), and P-glycoprotein (Pgp/ABCB; reviewed in Borst and Elferink, 2002; Haimeur et al., 2004; Ambudkar et al., 2003; Gottesman et al., 2002). Overexpression of these multidrug resistance (MDR) efflux transporters results in an ATP-dependent decrease in drug accumulation in various malignant cells (and Elferink, 2002; Haimeur et al., 2004; Doyle et al., 2003; Ambudkar et al., 2003; Gottesman et al., 2002). Consequently, overexpression of MRP1, BCRP or Pgp results in the acquisition of MDR to multiple anticancer drugs. Increased expression of MRP1, Pgp and BCRP has been documented in hematological malignancies and solid tumors, suggesting an important role for these transporters in the potential conferring of clinical drug resistance upon malignant cells (Doyle et al., 2003; Gottesman et al., 2002; Leonard et al., 2003; Nakanishi et al., 2003).

Apart from their protective role against various xenobiotics, some ABC transporters are able to mediate the ATP-driven export of non-toxic endogenous substrates. To date, four efflux transporters including MRP1 through MRP4 have been shown to mediate the efflux of monoglutamates of folates (reviewed in Borst and Elferink, 2002; Haimeur et al., 2004; Doyle et al., 2003). Reduced folate cofactors play a pivotal role in various one-carbon transfer reactions in the *de novo* biosynthesis of purines and thymidylate and are therefore essential for DNA replication (Stockstad, 1990). Hence, intracellular folate pools must be controlled such that they

can sustain a proper intracellular nucleotide pool that will allow for DNA synthesis. In contrast to MRP1 through MRP4, breast cancer resistance protein (BCRP/ABCG2) has the unique facility to extrude mono, di and tri-glutamates of folates and methotrexate (Chen et al., 2003; Volk and Schneider, 2003). Therefore, we recently initiated studies aimed at exploring the possible involvement of BCRP in the maintenance of cellular folate homeostasis. Toward this end, we found recently that *long-term* gradual deprivation of folates from the growth medium of cultured breast cancer cells with moderate (MCF-7) or high (MCF-7/MR) levels of BCRP resulted in the near complete loss of BCRP expression along with a marked decrease in MRP1 levels (Ifergan et al., 2004). This was also associated with an increased activity of folylpoly- γ -glutamate synthetase (FPGS), the enzyme responsible for folate retention via polyglutamylation. Consequently, these folate-deprived cells displayed a prominently diminished Hoechst 33342 efflux activity that was accompanied by a markedly increased sensitivity to both MR and methotrexate. Furthermore, these long-term folate-deprived cells accumulated significantly more radiolabeled folic acid than their parental counterparts that grew on medium containing high concentrations of folic acid. Hence, these results suggested that down-regulation of BCRP and MRP1 expression along with increased FPGS activity are apparently essential components of cellular adaptation to *long-term* folate deprivation. Based on these findings, we here subjected BCRP-overexpressing MCF-7/MR breast cancer cells to *short-term* folate deprivation. This resulted in a nearly complete lack of targeting of BCRP to the plasma membrane with a predominant localization of BCRP to the cytoplasmic compartment. In contrast, various transmembrane proteins retained their plasma membrane localization in the folate-deprived cells. Folate deprivation was also associated with a 3-fold decrease in BCRP and MRP1 levels. Subcellular immunofluorescence studies with these folate-deprived cells revealed that cytoplasmic BCRP co-localized with calnexin, an established endoplasmic reticulum (ER)

MOL # 8250

marker. Importantly, the loss of BCRP from the plasma membrane in folate-deprived cells resulted in a 6-fold increase in [^3H]folic acid accumulation, relative to cells grown in high folic acid medium. These results constitute a novel mechanism of cellular adaptation to short-term folate deprivation and provide further support to the ability of BCRP to modulate cellular folate pools.

Materials and Methods

Chemicals: Folic acid, tunicamycin, triton X-100, tween 20, rhodamine 123, 3,3'-diaminobenzidine tetrahydrochloride, propidium iodide, 4,6-diamidino-2-phenylindole hydrochloride (DAPI), emetine hydrochloride and haematoxylin were obtained from Sigma Chemical Co. (St. Louis, MO). Mitoxantrone (MR) hydrochloride was from Cyanamid of Great Britain Ltd (Gosport, Hampshire, England).

Tissue culture: The MR-resistant human breast cancer cell line MCF-7/MR (originally termed MCF-7/Mitox; see Taylor et al., 1991) with BCRP overexpression (Ifergan et al., 2004) was grown under monolayer conditions in RPMI-1640 medium containing 2.3 μ M folic acid (Biological Industries, Beth-Haemek, Israel), 10% fetal calf serum (GIBCO), 2 mM glutamine, 100 μ g/ml penicillin and 100 μ g/ml streptomycin. Once every two weeks, MCF-7/MR cells were cultured in the presence of 0.1 μ M MR. The human ovarian carcinoma 2008/MRP1 subline, stably transduced with an MRP1 cDNA (kindly provided by Prof. P. Borst, The Netherlands Cancer Institute, Amsterdam, The Netherlands) was cultured in the above RPMI-1640 medium. The Emt^{R1} Chinese hamster ovary cell line was derived in our lab by stepwise selection in increasing concentrations of emetine resulting in stable Pgp overexpression (Borgnia et al., 1996). This cell line was routinely grown in RPMI-1640 medium supplemented with 1 μ M emetine.

Western blot analysis of BCRP, MRP1 and Pgp expression: To examine the expression of BCRP, MRP1 and Pgp in the various cell lines, non-ionic detergent-soluble membrane proteins were extracted as previously described (Ifergan et al., 2004). Proteins (10-20 μ g) were resolved by electrophoresis on 10% (for BCRP) or 7% (for MRP1 or Pgp) polyacrylamide gels containing SDS and electroblotted onto Protran BA83 cellulose nitrate membranes (Schleicher & Schuell, Dassel, Germany). The blots were blocked for 1 hr at room temperature in TBS

buffer (10 mM Tris pH 8.0, 150 mM NaCl and 0.5% Tween 20) containing 1% skim milk. The blots were then reacted with the following anti-human BCRP, MRP1 and Pgp monoclonal antibodies (generously provided by Prof. R.J. Scheper and Dr. G.L. Scheffer VU University Medical Center, Amsterdam, The Netherlands): BXP-53, a rat anti-BCRP antibody (at a dilution of 1:1000); MRP-r1, a rat anti-MRP1 antibody (1:1,000) and JSB-1, a mouse anti-Pgp antibody (1:100). Blots were then rinsed in the same buffer for 10 min at room temperature and reacted with second antibodies consisting either of horseradish peroxidase (HRP)-conjugated goat anti-mouse or anti-rat IgG (1: 10,000 dilution, Jackson ImmunoResearch Labs, West Grove, PA) for 1 hr at room temperature. Following three washes (each of 10 min) in TBS at room temperature, enhanced chemiluminescence (ECL) detection was performed according to the manufacturer's instructions (Biological Industries, Beth-Haemek, Israel). To normalize for loading differences, the blots were first stripped using the following procedure: incubation for 10 min in a stripping solution containing 0.5 M NaCl, 0.5M acetic acid at pH 2.4. The nylon membranes were then washed twice with TBS and reacted with an antibody against β -tubulin, clone 2-28-33 from Sigma (1: 4,000).

Immunohistochemistry studies: Cells (5×10^4) from each cell line were seeded in 25-mm tissue culture flasks and incubated for 4 days in 5 ml of growth medium. Monolayer cells were then washed twice with PBS and fixed for 10 min in a solution of 4% formaldehyde in PBS.

Endogenous peroxidase activity was neutralized by incubation for 20 min in a solution consisting of 4 volumes of methanol and 1 volume of 3% H_2O_2 in double distilled water. The fixed cells were washed twice with PBS, blocked for 1 hr at room temperature in PBS containing 1% skim milk and reacted with the following antibodies: rat anti-human BCRP monoclonal antibody BXP-53 (1:100), mouse anti-human EGFR monoclonal antibody 111.6 (1:100, generously provided by Prof. Y. Yarden, The Weizmann Institute of Science, Rehovot,

Israel), rabbit polyclonal antibodies to human FGFR1 Flg (H-76), FGFR2 (Bek C-17) and FGFR3 (H-100; all at a 1:100 dilution; Santa Cruz Biotechnology, Santa Cruz, CA). Then, HRP-conjugated goat anti-rat, -mouse or -rabbit IgG (all at 1:100 dilution; Jackson ImmunoResearch Labs, West Grove, PA) were added followed by two washes with PBS. Color development was performed with the chromogen 3,3'-diaminobenzidine (0.6 mg/ml) in a solution containing 0.02% H₂O₂ at pH 7.6. Following counterstaining of nuclei with haematoxylin, cells were examined with an Olympus BH-2 upright light microscope at random monolayer positions avoiding the edges of the flasks.

Immunofluorescence analysis with viable cells: Cells (10⁴) from each cell line were seeded onto 24-well plates (1ml medium/well) on sterile glass coverslips and incubated for 4 days at 37°C. Then, the growth medium was removed and monolayer cells were washed twice with PBS and blocked for 1 hr at room temperature in PBS containing 10% fetal calf serum (GIBCO) and reacted with a mouse anti-MHC class I monoclonal antibody W6/32 (1:100, kindly provided by Prof. Yoram Reiter, Technion, Haifa, Israel) in a blocking solution for 45 min at room temperature. The coverslips were then washed twice with PBS and reacted in blocking solution with an FITC-conjugated goat anti-mouse antibody (1:100; Jackson ImmunoResearch Labs, West Grove, PA). Following 40 min of incubation at room temperature, the coverslips containing viable cells were washed twice with PBS, mounted onto glass slides and examined using a LEICA immunofluorescence microscope. We also performed a control experiment in which the mouse anti-MHC W6/32 monoclonal antibody was omitted.

Confocal and immunofluorescence microscopy studies with fixed cells: Cells (10⁴) from each cell line were seeded onto 24-well plates (1ml medium/well) on sterile glass coverslips and incubated for 4 days at 37°C. Then, the growth medium was removed and monolayer cells were washed twice with PBS and fixed with 4% formaldehyde in PBS for 10 min. The coverslips

MOL # 8250

were washed twice with PBS and then incubated for 20 min in a solution of 80% methanol in double distilled water. The coverslips were washed twice with PBS, blocked for 1 hr at room temperature in PBS containing 1% skim milk and reacted with a rat anti-BCRP monoclonal antibody BXP-53 (1:100) for 60 min at room temperature. The coverslips were washed twice with PBS and reacted with a goat anti-rat IgG (1:100) and mouse anti-calnexin antibody (1:100; Transduction Laboratories, catalogue # C45520) for 60 min at room temperature. After washing twice with PBS, the cells were incubated with the secondary FITC-conjugated rabbit-anti-goat IgG (1:100; Sigma; catalogue # D-9564) and Cy3-conjugated donkey-anti-mouse IgG (1:100; Cat # 715-165-151; Jackson ImmunoResearch Labs, West Grove, PA). Cell nuclei were stained with the DNA dye DAPI (Sigma; catalogue # D-9564) at a final concentration of 0.5 µg/ml for 60 min at room temperature. Following four washes with PBS (each with 2 ml), the coverslips were mounted onto glass slides using fluoromount-GTM (Southern Biotech; catalogue # 0100-01). The slides were then examined using a LEICA immunofluorescence microscope and a BioRad MRC1024 confocal microscope.

Propidium iodide staining and cell cycle analysis: Monolayer cells were detached by trypsinization, adjusted to a density of 10^6 cells/ml in PBS, fixed with 70% ethanol and stained with propidium iodide (PI) as previously described (Darzynkiewicz et al., 1994). PI-stained cells were then analyzed by flow cytometry using a 488 nm laser excitation and emission was collected at 585 nm. The percentages of cells at apoptosis or with a >4n DNA content were calculated using a WinMDI software (version 2.8).

Assay of cellular rhodamine 123 accumulation: Cells (5×10^4) from each cell line were seeded onto 25-mm tissue culture flasks for 4 days; the medium was replaced and allowed to equilibrate by 4 hr incubation at 37°C in an atmosphere of 5% CO₂. Then, rhodamine123 was added to the

growth medium at a final concentration of 750 nM. After 60 min of incubation at 37°C, monolayer cells in the tissue culture flasks were washed seven times with cold PBS (each time with 8ml/flask). In order to extract cellular rhodamine 123 fluorescence, cells were lysed with a solution of PBS containing 1% Triton X-100 (1.6 ml/flask). Total cellular fluorescence was determined in quartz cuvettes using a fluorescence spectrophotometer (CARY, Eclipse). The fluorescence readings were normalized to the relative number of cells present in each culture flask that were determined with duplicate flasks prior to rhodamine 123 accumulation. The entire rhodamine 123 accumulation study was carried out in the dark.

Quantitative analysis of the cytoplasmic and plasma membrane fractions of BCRP:

First, the immunohistochemical images were processed using adobe photoshop software (version 6.0), and only the brown diaminobenzidine color corresponding to the BCRP staining was selected automatically and then copied to a new picture with a white background. All the other accompanying colors including that of the counterstain hematoxylin were excluded. This new image represented total cellular BCRP staining. In order to obtain a picture representing the cytoplasmic BCRP staining, the original pictures were opened once again using adobe photoshop software followed by manual erasure of the plasma membrane staining. Then, the brown BCRP staining was selected automatically and copied to yield a new picture of the cytoplasmic staining. Total staining and cytoplasmic staining was transformed to a grayscale picture and analyzed separately by scanning densitometry using the program "TINA" (version 2.10g). The local background levels were subtracted from the original densitometric values resulting in two corrected values for each colony: total cellular staining of BCRP and cytoplasmic BCRP staining. The percentage of the cytoplasmic fraction was obtained by dividing the value of cytoplasmic BCRP staining by that of the total cellular BCRP staining, multiplied by 100.

[³H]Folic acid accumulation: Adherent cells (~8x10⁶) in T75 tissue culture flasks (Nunc) were washed with HBS, detached by trypsinization and suspended at 10⁷ cells/ml in the same buffer as described previously (Ifergan et al., 2004). [³H]folic acid (69 Ci/mmol, Moravek Biochemicals, Brea, CA) was added to a final concentration of 2 μM (specific radioactivity 2,500 dpm/pmol) and incubated at 37°C for 30 min; 1 μM trimetrexate was included in order to block folic acid reduction (Assaraf and Goldman, 1997). Transport was terminated and cells were processed for scintillation counting as described previously (Ifergan et al., 2004).

Statistical Analysis: We used a one-tailed student's T-test to examine the significance of the difference between two populations for a certain variable. A difference between the averages of two populations was considered significant if the P-value obtained was < 0.05.

Scanning densitometry: Relative BCRP and MRP1 protein levels were determined by scanning densitometry of several linear exposures using the program "TINA" (version 2.10g) divided by the densitometrical value of β-tubulin.

Results

Establishment of a short-term folate deprivation protocol: Recently we have shown that *long-term* gradual deprivation of folic acid from the growth medium resulted in the near complete loss of BCRP expression along with a marked decrease in MRP1 expression in MR-resistant MCF-7/MR breast cancer cells (Ifergan et al., 2004). Here we explored the mode of adaptation of these BCRP-overexpressing cells upon a *short-term* deprivation of folic acid from the growth medium. Toward this end we established a *short-term* folate deprivation protocol (**Fig 1**). Briefly, MCF-7/MR cells growing in a high folic acid (2.3 μ M) medium containing MR were washed with excess PBS and distributed to three groups; one group continued to grow in the above medium and was termed MCF-7/MR-HF-MR, whereas the second group was grown in drug-free medium containing high folic acid and was therefore termed MCF-7/MR-HF. The third group which was termed MCF-7/MR-NF-LF was grown for two weeks in folic acid-free medium (i.e. the folate deprivation step) followed by an additional week of adaptation to low folic acid (1 nM). At the end of this three weeks period, cells from the various groups were processed for various analyses. In order to confirm that folate-deprived MCF-7MR-NF-LF cells retained normal cell cycle kinetics, we performed a flow cytometric analysis with propidium iodide-stained cells. Folate-deprived cells displayed a normal cell cycle distribution in the G₁, S and G₂M phases, when compared to the control groups growing in high folate medium (**Fig 2**). Furthermore, in the group of folate-deprived cells, the apoptotic/dead cell fraction was relatively small ($8.1 \pm 0.5\%$) and was similar to that obtained with control cells growing in high folate medium ($8.8 \pm 0.5\%$). As would be expected, MCF-7/MR-HF-MR cells growing in a medium containing the cytotoxic drug MR displayed a slight increase in the fraction of apoptotic cells ($13.2 \pm 0.1\%$). Furthermore, the percentage of cells with >4n DNA content in MCF-7/MR-HF-MR and MCF-7/MR-HF cells were comparable 21.9 ± 1.9 and 20.2 ± 1.7 , respectively, whereas

the MCF-7/MR-NF-LF subline had a lower fraction of cells with a $>4n$ DNA content (11.2 ± 3.2 %). These results are consistent with the well established genomic instability and chromosomal aberrations of cultured tumor cell lines.

Expression and Glycosylation of BCRP in short-term folate deprived cells and their

control counterparts: As we have recently shown that *long-term* folate-deprivation results in a dramatic loss of BCRP and MRP1 expression (Ifergan et al., 2004), we first determined the status of expression of these transporters in short-term folate-deprived cells. Western blot analysis with monoclonal antibodies to BCRP (**Fig 3A,B**) and MRP1 (**Fig 3C**) revealed a 3-fold decrease in their levels in folate-deprived cells relative to parental cells growing in a high folate medium (**Fig 3A-C**). Since two closely migrating BCRP species were apparent in both MCF-7/MR-NF-LF cells and their parental MCF-7/MR counterparts (**Fig 3A**), we undertook experiments in order to rule out the possibility that folate-deprivation results in alterations in BCRP glycosylation. Thus, MCF-7/MR-NF-LF cells and their parental MCF-7/MR counterparts were treated with the *N*-glycosylation inhibitor tunicamycin (10 μ g/ml) for 24 hr, following which Western blot analysis was performed with a monoclonal antibody to BCRP (**Fig 3B**). The completely unglycosylated BCRP in all tunicamycin-treated cell lines migrated as a faint ~ 72 kDa protein thereby being much lower in its molecular mass than either of the two glycosylated high molecular weight BCRP bands (~ 80 kDa and 82 kDa, respectively). Hence, the ~ 80 kDa and 82 kDa BCRP species observed in equal ratios in both MCF-7/MR-NF-LF and MCF-7/MR cells are both glycosylated but to slightly different extents, whereas the unglycosylated BCRP obtained after treatment with tunicamycin has a much lower molecular mass as would be predicted from the calculated core molecular mass of BCRP. Hence, short-term folate deprivation does not alter the glycosylation of BCRP. Reprobing with a β -tubulin antibody confirmed that equal amounts of proteins were analyzed (**Fig 3E**).

Subcellular localization of BCRP in short-term folate deprived cells and their control

counterparts: Previously we have shown that relative to their parental MCF-7 cells, MCF-7/MR cells display a ~55-fold BCRP overexpression, the large fraction of which is in the plasma membrane (Ifergan et al., 2004). Hence, the surprisingly modest decrease in BCRP and MRP1 levels in the short-term folate deprived cells here could not account for their survival under folate-deficient conditions when taking into consideration the potent folate efflux activity of BCRP in MCF-7/MR cells (Chen et al., 2003; Volk and Schneider, 2003; Ifergan et al., 2004). Therefore, we further explored the expression and subcellular localization of BCRP in these cells by immunohistochemistry. MCF-7/MR-HF-MR and MCF-7/MR-HF cells growing in high folic acid medium displayed an intense plasma membrane staining of BCRP, particularly at zones of cell-cell adhesion (**Fig 4A,B**, upper panel, see *arrows*). In contrast, in folate-deprived cells, BCRP was highly confined to the cytoplasm (**Fig 4C**, *dashed arrows*). These results were corroborated with immunofluorescence analysis of cells stained with DAPI, a DNA dye with a blue fluorescence. Thus, the green fluorescence of BCRP clearly localized to zones of cell-cell attachment in MCF-7/MR-HF-MR and MCF-7/MR-HF cells as aided by the blue fluorescence of the nuclei (**Fig 4A,B**, lower panel). In contrast, BCRP was confined to the cytoplasm in folate-deprived cells (**Fig 4C**, lower panel). Furthermore, detailed time-course experiments revealed that the first significant appearance of the cytoplasmic BCRP localization was observed only after two weeks of folate deprivation followed by at least 4 additional days of adaptation in 1 nM folic acid-containing medium.

In order to provide a quantitative assessment of this markedly altered subcellular distribution, we devised a computerized whole-cell scanning technique (see Materials and Methods) and thereby determined the percentage of BCRP in the cytoplasm and plasma membrane fractions in the various cell lines after immunohistochemical staining with an anti-

BCRP antibody. MCF-7/MR-HF-MR cells contained $70 \pm 9.8\%$ of their BCRP in the plasma membrane and only $30 \pm 9.8\%$ in cytoplasm, whereas folate-deprived cells contained $86 \pm 1.7\%$ of their BCRP in the cytoplasm and only $14 \pm 1.7\%$ in the plasma membrane (**Fig 5A**); this dramatic increase in the cytoplasmic fraction in folate-deprived cells was statistically significant ($P=0.002$). Furthermore, whereas the cytoplasmic/plasma membrane distribution ratio of BCRP in parental MCF-7/MR-HF-MR cells was 0.65 ± 0.28 , folate-deprived cells had a statistically significant, ~ 9.3 -fold increase in this ratio (6.06 ± 0.84 ; $P=0.001$; **Fig 5B**). These results establish that BCRP is highly confined to the cytoplasm in the short-term folate-deprived cells.

Retention of plasma membrane localization of various membrane proteins in the short-term folate-deprived cells: In order to determine whether short-term folate-deprivation results in a selective cytoplasmic localization of BCRP, we performed immunohistochemistry experiments with antibodies directed to various plasma membrane proteins including epidermal growth factor receptor (EGFR) as well as fibroblast growth factor receptor 1 (FGFR1), FGFR2 and FGFR3. We also undertook immunofluorescence studies with viable cells using a monoclonal antibody to an external epitope of MHC class I. Albeit these membrane proteins were expressed at variable levels, both EGFR (**Fig 6A**), FGFR1 (**Fig 6B**), FGFR2 (**Fig 6C**), FGFR3 (**Fig 6D**) and MHC class I (**Fig 6E**) retained their normal plasma localization in folate-deprived cells as in their parental cells. These results strongly suggest that the cytoplasmic localization of BCRP in the short-term folate-deprived cells is specific to BCRP as various transmembrane proteins retained their normal plasma membrane localization.

Co-localization of BCRP in the ER compartment in folate-deprived cells: In order to better define the cytoplasmic sub-cellular localization of BCRP in folate-deprived cells, we used confocal microscopy after immunostaining; cells were stained either with anti-BCRP antibodies followed by an FITC-conjugated antibody (i.e. green fluorescence, **Fig 7A**), or with anti-

calnexin, an established endoplasmic reticulum resident (Baron et al., 2003; Kleizen and Braakman, 2004) followed by a Cy 3-conjugated antibody (red fluorescence, **Fig 7B**). Cell nuclei were counterstained with the DNA dye, DAPI (blue fluorescence, **Fig 7C**). MCF-7/MR-HF-MR and MCF-7/MR-HF cells displayed an intense green fluorescence (i.e. BCRP) at the plasma membrane, particularly at cell-cell contact zones (**Fig 7A**). In contrast, folate-deprived MCF-7/MR-NF-LF cells had a green cytoplasmic BCRP fluorescence with no detectable plasma membrane staining (**Fig 7A**). In all cell lines, the red fluorescence derived from the anti-calnexin antibodies was highly confined to the perinuclear region (**Fig 7B**) as would be expected from an ER marker (Baron et al., 2003; Kleizen and Braakman, 2004). The DAPI-stained nuclei with blue fluorescence served to localize the perinuclear ER staining (**Fig 7C**). Remarkably, merging the green BCRP fluorescence and the red calnexin fluorescence in the folate-deprived cells revealed a perfect perinuclear co-localization as evidenced by the resultant yellow color (**Fig 7D**). In contrast, merging the green BCRP fluorescence and the red calnexin fluorescence did not result in any substantial ER co-localization in MCF-7/MR-HF-MR and MCF-7/MR-HF cells. These results establish that BCRP is highly confined to the ER compartment in folate-deprived cells.

Functionality of BCRP in the various cell lines: in order to determine whether the loss of BCRP from the plasma membrane of folate-deprived cells was accompanied by a parallel loss of a plasma membrane efflux function, we measured rhodamine 123 accumulation in these cells. Rhodamine 123 was shown to be a moderate transport substrate of R482 BCRP and an excellent substrate of G482 BCRP (Robey et al., 2003). Rhodamine 123 was also shown to be an efflux substrate of Pgp (Assaraf and Borgnia, 1994); however, as shown in **Fig 3D**, MCF-7/MR-HF-MR cells and their sublines were completely devoid of Pgp. Cells were incubated for 1 hr in the presence of 0.75 μ M rhodamine 123 after which cell-associated dye was extracted and

determined spectrofluorometrically. Folate-deprived cells accumulated 3-fold more rhodamine 123 when compared with control cells grown in medium containing high folates (**Fig 8**); this increased rhodamine 123 accumulation in folate-deprived cells was statistically significant ($P=0.017$). Thus, the loss of BCRP from the plasma membrane in folate-deprived cells was accompanied by an increased cellular accumulation of rhodamine 123. Consistently, MCF-7/MR-NF-LF cells who had a cytoplasmic to plasma membrane BCRP distribution ratio of ~ 6 (**Fig 5B**), consistently displayed a 4.5-fold increased [^3H]folic acid accumulation (**Fig 9**), when compared to MCF-7/MR cells that contained most of their BCRP in the plasma membrane ($P=0.0026$). These results provide strong evidence that the cytoplasmic confinement of BCRP in the short-term folate-deprived cells serves a functional role of markedly augmenting cellular folate accumulation. Hence, in order to explore the possibility of whether the confinement of BCRP to the cytoplasm under conditions of folate deprivation is correlated with cell growth or the number of cells in the colony, we plotted the percentages of cytoplasmic BCRP versus the number of cells in the different colonies for each cell line (**Fig 10**). Remarkably, in the folate-deprived cells (**Fig 10C**), the percentages of cytoplasmic BCRP were significantly higher in the colonies containing high cell numbers (i.e. cell number per colony $>$ the median cell number of the colonies in the population) than colonies containing low cell numbers (cell number per colony $<$ the median cell number of the colonies; $P=0.013$). In contrast, the MCF-7/MR-HF-MR (**Fig 10A**) and MCF-7/MR-HF (**Fig 10B**) cell lines failed to reveal any significant difference in the percentages of cytoplasmic BCRP when comparing the group of colonies containing high cell numbers and the group of colonies containing low cell numbers ($P=0.19$ and $P=0.76$, respectively).

Discussion

We have shown recently that *long-term* gradual deprivation of folic acid from the growth medium of breast cancer cells with BCRP overexpression results in almost a complete loss of BCRP expression along with a marked decrease in MRP1 levels (Ifergan et al., 2004). Here we studied the impact of *short-term* folic acid deprivation on BCRP expression, subcellular localization and efflux function. The rationale behind these experiments was that as BCRP has the facility to export mono-, di-, and triglutamates of folates (Chen et al., 2003; Volk and Schneider, 2003), the localization of an overexpressed BCRP at the plasma membrane should not be retained under conditions of folate deprivation. The following line of evidence confirms that the plasma membrane localization of BCRP has been lost in breast cancer cells subjected to a short-term folate-deprivation. First, immunohistochemistry revealed that although high levels of BCRP were retained, this transporter was confined to the cytoplasm rather than to the plasma membrane. Second, confocal microscopy after immunofluorescent staining with antibodies to BCRP as well as to calnexin, an established marker of the endoplasmic reticulum (ER) (Baron et al., 2003; Kleizen and Braakman, 2004), showed that BCRP was largely confined to the ER compartment in folate-deprived cells. This was inferred from BCRP colocalization with the ER resident calnexin. The latter is a lectin chaperone that functions in the quality control system in the ER (Kleizen and Braakman, 2004). Third, folate-deprived cells with a cytoplasmic to plasma membrane BCRP distribution ratio of 6, displayed a consistent increase (4.5-fold) in [³H]folic acid accumulation, when compared to their parental cells that contained most of their BCRP in the plasma membrane. Fourth, loss of BCRP from the plasma membrane was accompanied by a prominent increase in the cellular accumulation of rhodamine 123, a moderate R482 BCRP substrate (Robey et al., 2003). Since MCF-7/MR-HF-MR cells were devoid of Pgp which also exports rhodamine 123 (Assaraf and Borgnia, 1994), it was likely that the lack of sorting of

BCRP to the plasma membrane would result in increased rhodamine 123 accumulation in these folate-deprived cells. These data suggest that short-term folic acid deprivation presumably selects for the lack of plasma membrane targeting of BCRP, thereby resulting in the cytoplasmic confinement of this ABC transporter. Overexpressed BCRP with a cytoplasmic residence rather than the normal plasma membrane localization (Maliepaard et al., 2001) is a useful strategy aimed at eliminating the BCRP-dependent efflux of intracellular mono- and polyglutamates of folates. This would result in the preservation of the precious cellular folate pools that are particularly shrunken under conditions of folate deficiency (Rothem et al., 2002; Liani et al., 2003; Assaraf et al., 2003). Indeed, as mentioned above, short-term folate deprived cells had a drastic increase in the accumulation of [^3H]folic acid relative to their parental counterpart. Taken collectively, our previous study (Ifergan et al., 2004) demonstrates that *long-term* gradual folate deprivation results in the near complete loss of BCRP expression and a marked decrease in MRP1 levels. Whereas our current findings show that *short-term* folate deprivation leads to lack of plasma membrane targeting of BCRP and its cytoplasmic confinement, along with a moderate decrease in BCRP and MRP1 levels. We conclude that cytoplasmic confinement and decreased expression of BCRP are important components of cellular adaptation to *short-term* folate deprivation.

The present immunohistochemistry and immunofluorescence data suggest that folate-deprivation resulted in a cytoplasmic confinement of BCRP that appeared to be selective for this transmembrane protein. This is based upon the finding that various membrane proteins that are expressed at variable levels in breast cancer cells including EGFR, FGFR1,2,3 and MHC class I retained their dominant plasma membrane localization under conditions of folate-deprivation. As we show here that the cytoplasmic confinement of BCRP is not shared with various plasma membrane proteins, the phenomenon of plasma membrane confinement cannot be regarded as a

pleiotropic effect of folate-deprivation such that it would encompass various transmembrane proteins. Hence, these results suggest that the selective confinement of BCRP to the cytoplasmic compartment plays a contributing role in the cellular adaptation to conditions of folate deprivation.

Several possibilities exist that can provide a potential molecular basis for the novel finding of the cytoplasmic confinement of BCRP upon short-term folate deprivation. The first involves a recent paper (Mogi et al., 2003) that reported on the rapid translocation of BCRP from the plasma membrane to the cytoplasmic compartment in hematopoietic stem cells known as side population (SP); these cells are defined by the efflux of Hoechst 33342, an established BCRP substrate. In this study it was shown that a brief treatment (1.5 hrs) of freshly derived mouse bone marrow cells with LY294002, an inhibitor of the Akt effector protein phosphatidylinositol-3-kinase (PI3K), resulted in the translocation of BCRP from the plasma membrane to the cytoplasmic compartment. The authors therefore suggested that the PI3K-Akt signaling axis is an important regulator of BCRP expression and subcellular localization as well as of the bone marrow-derived SP stem cell phenotype. Thus, it is possible that the confinement of BCRP to the cytoplasmic compartment in our short-term folate-deprived breast cancer cells may be a result of the loss of activity of a component in the PI3K-Akt signaling pathway. However, it should be noted that in the current study, 1.5 hr treatment of MCF-7/MR cells with LY294002 did not result in a rapid translocation of BCRP from the plasma membrane to the cytoplasmic compartment. Thus, one cannot exclude the possibility of a longer term effect of this inhibitor on the cytoplasmic confinement of BCRP in breast cancer cells with BCRP overexpression. In support of this hypothesis, it has been shown that the PI3K-Akt signaling pathway controls the cellular localization of a number of proteins including GLUT4, an insulin-stimulated glucose transporter; this cytoplasmic localization involved the cycling of GLUT4

between the plasma membrane and specialized intracellular vesicles (Foster et al., 2001). In this regard, it has been shown recently that lung SP progenitor cells express BCRP on their surface, whereas muscle SP cells express intracellular BCRP and are therefore incapable of Hoechst 33342 efflux (Summer et al., 2003). Further, phosphoinositol 3,4-biphosphate enhanced the ATP-dependent transport of taurocholate in canalicular membrane vesicles *in vitro* and *in vivo* (Misra et al., 1998). Hence, it appears that the PI3K-Akt signaling pathway can alter the subcellular localization of membrane transporters and, through its lipid products it can directly modulate the transport activity of membrane transporters including the Mdr1 and Mdr2 gene products. The second possibility involves a recent paper in which the impact of BCRP mutations and single amino acid polymorphisms on its localization, ATPase activity and efflux function was explored (Mizuarai et al., 2004). It was found that an N-terminal BCRP mutation (Val12Met) disrupted the apical plasma membrane localization of BCRP in polarized LLC-PK1 cells. The third possibility involves the use of a BCRP that was tagged with a cyan green fluorescent protein and then transiently expressed in HeLa cells (Rajagopal and Simon, 2003). In this study it was found that BCRP colocalized to a perinuclear compartment that was positive for lysosomal markers including cathepsin D and synaptotagmin VII. The authors therefore suggested that BCRP can display a variable subcellular localization other than the plasma membrane in different cell lines and under different conditions. Consistent with our current findings, these results establish that BCRP has the inherent capability to be localized at certain cytoplasmic compartments including ER and lysosomes.

The cytoplasmic localization of BCRP in folate-deprived cells has potentially important implications for combination chemotherapy. BCRP has been shown to confer resistance to various anticancer drugs including doxorubicin, mitoxantrone, topotecan, and the antifolate methotrexate (Robey et al., 2003; Sarkadi et al., 2004). Hence, chemotherapeutic regimens

containing some of these BCRP efflux substrates including the CAF and CMF protocols which contain cyclophosphamide, adriamycin (i.e. doxorubicin), 5-fluorouracil and methotrexate for the treatment of breast cancer may become limited in their efficacy if BCRP is overexpressed in these malignant cells (Borst and Elferink, 2002; Haimeur et al., 2004; Doyle et al., 2003; Gottesman et al., 2002; Leonard et al., 2003; Sarkadi et al., 2004). As such, one potential strategy to overcome BCRP-dependent drug-resistance may be the use a combined treatment of cancer cells with trimetrexate, a lipid-soluble analogue of methotrexate that is not recognized by BCRP as an efflux substrate (A. Shafran and Assaraf, Y.G, unpublished data) along with conventional chemotherapeutic drugs including cyclophosphamide and 5-fluorouracil. This antifolate treatment should result in an intracellular folate depletion thereby resulting in the possible confinement of BCRP to the cytoplasmic compartment aimed at preserving cellular folates. The resultant breast cancer cells should be vulnerable and could be easily eradicated even with chemotherapeutic drugs that are BCRP substrates (e.g. mitoxantrone and topotecan), as no plasma membrane BCRP efflux would be operable. An alternative approach would be pulse-treatment of BCRP overexpressing cancer cells with a PI3K inhibitor like LY294002 (Mogi et al., 2003). This could possibly lead to the confinement of BCRP to the cytoplasmic compartment thereby achieving reversal of the MDR phenotype as would be obtained with specific BCRP efflux inhibitors like Ko143 (Allen et al., 2002). Clearly, these potential strategies to overcome BCRP-dependent drug resistance must await further studies in order to explore their feasibility and potential applicability.

In the present paper we note that the cytoplasmic confinement of BCRP was much more pronounced ($P=0.013$) in large colonies (i.e. colony number greater than the median) than in small colonies (i.e. colony number lower than the median) of folate-deprived cells. Hence, it is very likely that during the short-term folate-deprivation, clonal sub-populations with a dominant

cytoplasmic BCRP localization may have gained a significant growth advantage over subpopulations with high plasma membrane fraction but low cytoplasmic confinement. This presumed growth advantage is based upon the fact that the loss of BCRP from the plasma membrane would lead to a parallel loss of efflux of cellular folates as evidenced by the drastic increase in [³H]folic acid accumulation in both short-term (the present study) and long-term folate deprived cells (Ifergan et al., 2004). Consequently, cells within colonies that display a dominant cytoplasmic BCRP localization could better preserve their intracellular folate pools thereby leading to a growth advantage as reflected in the increased number of cells per colony.

Acknowledgments

We thank Prof. R.J. Scheper and Dr. G.L. Scheffer for generously providing us with monoclonal antibodies to BCRP, MRP1 and Pgp and Dr. A.H. Schinkel for the kind gift of Ko143. We extend our gratitude to Prof. Y. Yarden for the EGFR monoclonal antibody as well as to Prof. Y. Reiter for the MHC class I monoclonal antibody.

References

Allen JD, van Loevezijn A, Lakhai JM, van der Valk M, van Tellingen O, Reid G, Schellens JH, Kooman GJ, and Schinkel AH (2002) Potent and specific inhibition of the breast cancer resistance protein multidrug transporter in vitro and in mouse intestine by a novel analogue of fumitremorgin C. *Mol Cancer Ther* 1: 417-425.

Ambudkar SV, Kimchi-Sarfaty C, Sauna ZE, and Gottesman MM (2003) P-glycoprotein: from genomics to mechanism. *Oncogene* 22: 7468-7485.

Assaraf YG, and Borgnia MJ (1994) Probing the interaction of the multidrug-resistance phenotype with the polypeptide ionophore gramicidin D via functional channel formation. *Eur J Biochem* 212: 813-824.

Assaraf YG, Rothem L, Hooijberg JH, Stark M, Ifergan I, Kathmann IA, Dijkmans BAC, Peters GJ, and Jansen G (2003) Loss of multidrug resistance protein 1 expression and folate efflux activity results in a highly concentrative folate transport in human leukemia cells. *J Biol Chem* 278: 6680-6686.

Assaraf YG, and Goldman, ID (1997) Loss of folic acid exporter function with markedly augmented folate accumulation in lipophilic antifolate-resistant mammalian cells. *J Biol Chem* 272: 17460-17466.

Baron D, Assaraf YG, Cohen N, and Aronheim A (2003) Lack of plasma membrane targeting of a G172D mutant thiamine transporter derived from Rogers syndrome family. *Mol Med* **8**: 463-475.

Borgnia MJ, Eytan GD, and Assaraf YG (1996) Competition of hydrophobic peptides, cytotoxic drugs, and chemosensitizers on a common P-glycoprotein pharmacophore as revealed by its ATPase activity. *J Biol Chem* **271**: 3163-3171.

Borst P and Elferink RO (2002) Mammalian ABC transporters in health and disease. *Annu Rev Biochem* **71**: 537-592.

Chen Z-S, Robey RW, Belinsky MG, Schvaveleva I, Ren XO, Sugimoto Y, Ross DD, Bates SE, and Kruh GD (2003) Transport of methotrexate, methotrexate polyglutamates, and 17beta-estradiol 17-(beta-D-glucuronide) by ABCG2: effects of acquired mutations at R482 on methotrexate transport. *Cancer Res* **63**: 4048-4054.

Cole SP, Bhardwaj G, Gerlach JH, Mackie JE, Grant CE, Almquist KC, Stewart A J, Kurz EU, Duncan AM, and Deeley RG (1992) Overexpression of a transporter gene in a multidrug-resistant human lung cancer cell line. *Science* **258**: 1650-1654.

Darzynkiewicz Z, Li X, and Gong J. (1994) Assay of cell viability: discrimination of cells dying by apoptosis. *Methods Cell Biol* **41**: 15-38.

Doyle LA and Ross DD (2003) Multidrug resistance mediated by the breast cancer resistance protein BCRP (ABCG2). *Oncogene* **22**:7340-7358.

Foster LJ, Li D, Randhawa VK, and Klip A (2001) Insulin accelerates inter-endosomal GLUT4 traffic via phosphatidylinositol 3-kinase and protein kinase B. *J Biol Chem* **276**: 44212-44221.

Gottesman MM, Fojo T, and Bates SE (2002) Multidrug resistance in cancer: role of ATP-dependent transporters. *Nat. Rev. Cancer* **2**: 48-58.

Haimeur A, Conseil G, Deeley RG, and Cole SP (2004) The MRP-related and BCRP/ABCG2 multidrug resistance proteins: biology, substrate specificity and regulation. *Curr Drug Metab* **5**: 21-53.

Ifergan I, Shafran A, Jansen G, Hooijberg JH, Scheffer GL, and Assaraf YG (2004) Folate deprivation results in the loss of breast cancer resistance protein (BCRP/ABCG2) expression. A role for BCRP in cellular folate homeostasis. *J Biol Chem* **279**: 25527-25534.

Kleizen B, and Braakman I (2004) Protein folding and quality control in the endoplasmic reticulum. *Curr Opin Cell Biol* **16**: 343-349.

Leonard GD, Fojo T, and Bates SE (2003) The role of ABC transporters in clinical practice. *Oncologist* **8**: 411-424.

Liani E, Rothem L, Bunni MA, Smith CA, Jansen G, and Assaraf YG (2003) Loss of folylpoly-gamma-glutamate synthetase activity is a dominant mechanism of resistance to polyglutamylation-dependent novel antifolates in multiple human leukemia sublines. *Int J Cancer* **103**: 587-599.

Maliepaard M, Scheffer GL, Faneyte IF, van Gastelen MA, Pijnenborg AC, Schinkel AH, van De Vijver RJ, and Schellens JH (2001) Subcellular localization and distribution of the breast cancer resistance protein transporter in normal human tissues. *Cancer Res* **61**: 3458-3464.

Misra S, Ujhazy P, Gatmaitan Z, Varticovski L, and Arias IM (1998) The role of phosphoinositide 3-kinase in taurocholate-induced trafficking of ATP-dependent canalicular transporters in rat liver. *J Biol Chem* **273**: 26638-26644.

Mizuarai S, Aozasa N, and Kotani H (2004) Single nucleotide polymorphisms result in impaired membrane localization and reduced ATPase activity in multidrug transporter ABCG2. *Int J Cancer* **109**: 238-246.

Mogi M, Yang J, Lambert JF, Colvin GA, Shiojima I, Skurk C, Summer R, Fine A, Quesenberry PJ, and Walsh K (2003) Akt signaling regulates side population cell phenotype via Bcrp1 translocation. *J. Biol. Chem.* **278**: 39068-39075.

MOL # 8250

Nakanishi T, Karp JE, Tan M, Doyle LA, Peters T, Yang W, Wei D, and Ross DD (2003) Quantitative analysis of breast cancer resistance protein and cellular resistance to flavopiridol in acute leukemia patients. *Clin Cancer Res* **9**: 3320-3328.

Rajagopal A, and Simon SM (2003) Subcellular localization and activity of multidrug resistance proteins. *Mol Cell Biol* **14**: 3389-3399.

Robey RW, Honjo Y, Morisaki K, Nadjem TA, Runge S, Risbood M, Poruchynsky, MS, and Bates SE (2003) Mutations at amino-acid 482 in the ABCG2 gene affect substrate and antagonist specificity. *Br J Cancer* **89**:1971-1978.

Rothem L, Ifergan I, Kaufman Y, Priest, DG, Jansen G, and Assaraf YG (2002) Resistance to multiple novel antifolates is mediated via defective drug transport resulting from clustered mutations in the reduced folate carrier gene in human leukaemia cell lines. *Biochem J* **367**: 741-750.

Sarkadi B, Ozvegy-Laczka C, Nemet K, and Varadi A (2004) ABCG2-a transporter for all seasons. *FEBS Lett* **67**: 116-120.

Stockstad ELR. Historical perspective on key advances in the biochemistry and physiology of folates. In: (Piccianno,M.F., Stockstad, E.L.R., Gregory, J.F. eds) Folic Acid Metabolism in Health and Disease. Wiley-Liss, New York, 1990, pp.1-21.

MOL # 8250

Summer R, Kotton DN, Sun X, Ma B, Fitzsimmons K, and Fine A (2003) Side population cells and Bcrp1 expression in lung. *Am J Physiol* **285**: L97-L104.

Taylor CW, Dalton WS, Parrish PR, Gleason MC, Bellamy WT, Thompson FH, Roe DJ, and Trent JM (1991) Different mechanisms of decreased drug accumulation in doxorubicin and mitoxantrone resistant variants of the MCF7 human breast cancer cell line. *Br J Cancer* **63**: 923-929.

Volk EL, and Schneider E (2003) Wild-type breast cancer resistance protein (BCRP/ABCG2) is a methotrexate polyglutamate transporter. *Cancer Res* **63**: 5538-5543.

Figure Legends

Fig 1: Schematic presentation of the short-term folate deprivation protocol. For details see the Results section.

Fig 2: Cell cycle analysis of folate-deprived cells and their control counterparts:

Following cell fixation with ethanol and staining with the DNA dye propidium iodide, cell cycle analysis was performed using a flow cytometer. The average fraction of apoptotic/dead cells (\pm S.D.) represented by a lower than G₁ DNA content is depicted for each cell line and has been obtained from three separate experiments.

Fig 3: Western blot analysis of BCRP, MRP1 and Pgp in folate-deprived cells and their control counterparts:

Triton X-100-soluble membrane proteins (20 μ g) were resolved by electrophoresis on polyacrylamide gels containing SDS, electroblotted onto Protran BA83 cellulose nitrate membranes and reacted with monoclonal antibodies against BCRP (A,B), MRP1 (C) or Pgp (D). Membrane proteins shown in panel B were isolated after 24 hr treatment of the various cell lines with 10 μ g/ml of the *N*-glycosylation inhibitor tunicamycin. Blots were then reacted with a second horseradish peroxidase (HRP)-conjugated antibody and these nylon membranes were developed using a standard ECL procedure. To correct for loading differences, the blots were stripped and reacted with an antibody against β -tubulin (E). The “overexpressor” lane contained protein extracts (6 μ g) from cell lines with overexpression of BCRP (MCF-7/MR), MRP1 (2008/MRP1) and Pgp (Emt^{R1}).

Fig 4: Immunohistochemical and immunofluorescence detection of BCRP in parental cells and their folate-deprived cells. *Upper Panel:* monolayer MCF-7/MR-HF-MR (A), MCF-7/MR-HF (B) and folate-deprived MCF-7/MR-NF-LF cells (C) were fixed with 4% formaldehyde and reacted with an anti-BCRP monoclonal antibody, BXP-53. Then, an HRP-

conjugated rabbit anti-rat IgG was added and color (brown) development was carried out using the chromogen 3,3'-diaminobenzidine. Cells were then counterstained with haematoxylin and examined with a light microscope at a 200x magnification. The *arrows* in A and B denote the plasma membrane localization of BCRP particularly at the region of cell-cell attachment in MCF-7/MR-HF-MR and MCF-7/MR-HF cells, respectively. Whereas, the *dashed arrow* represents the cytoplasmic localization of BCRP in folate-deprived MCF-7/MR-NF-LF cells (C). *Lower Panel:* Immunofluorescence detection with an FITC-conjugated antibody to BCRP (green fluorescence). Nuclei were counterstained with the DNA dye DAPI (blue fluorescence). Note the plasma membrane localization of BCRP in the region of cell-cell attachment in MCF-7/MR-HF-MR and MCF-7/MR-HF cells. Whereas, BCRP is confined to the cytoplasmic compartment in MCF-7/MR-NF-LF cells.

Fig 5: Histograms comparing the plasma membrane and cytoplasmic fractions of BCRP in folate-deprived cells and their control counterparts: Following

immunohistochemistry with a BCRP specific antibody, the percentage of the plasma membrane and cytoplasmic BCRP fractions were determined in the various cell lines (A) as detailed in Materials and Methods. The cytoplasmic/plasma membrane BCRP ratio in the various cell lines is also depicted (B); note the large increase in the cytoplasmic/plasma membrane BCRP ratio in the folate-deprived cells when compared to the control cells. Results depicted were obtained from three independent experiments in which a total number of ~1,200 cells from each cell line were processed for the determination of the plasma membrane and cytoplasmic BCRP fractions.

Fig 6: Immunohistochemistry and immunofluorescence localization of various plasma membrane proteins in folate-deprived cells and their parental counterparts: For immunohistochemistry studies, monolayer MCF-7/MR-HF-MR (left column), MCF-7/MR-

HF (middle column), and folate-deprived MCF-7/MR-NF-LF cells (right column) were fixed with 4% formaldehyde and reacted with antibodies to EGFR (A), FGFR1 (B), FGFR2 (C) and FGFR3 (D). Then, an HRP-conjugated goat anti-mouse or anti-rabbit IgG were added and color development was carried out using the chromogen 3,3'-diaminobenzidine. Cells were then counterstained with haematoxylin and examined with a light microscope at a 200x magnification. For immunofluorescence studies, viable cells were reacted with monoclonal antibodies to an external epitope of MHC class I (E) and a second FITC-conjugated goat anti-mouse antibody was added and cells were analyzed with a fluorescence microscope. For experimental details see Materials and Methods. The *arrows* denote the plasma membrane localization of the various membrane proteins.

Fig 7: Co-localization of BCRP in the ER compartment in folate-deprived cells as revealed by confocal microscopy: Monolayer cells growing on coverslips in 24-well plates were washed, fixed and reacted with monoclonal antibodies to BCRP (A) and calnexin (B) followed by counterstaining with the DNA dye DAPI (C). Then, FITC-conjugated antibodies (A, green fluorescence representing BCRP staining) and Cy3-conjugated antibodies (B, red fluorescence representing calnexin staining) were added. The merging of the green BCRP fluorescence with the red calnexin fluorescence is depicted in Panel D. Note that the merging of the green BCRP fluorescence and the red calnexin fluorescence in folate-deprived cells revealed a perinuclear ER co-localization as evidenced by the perinuclear yellow color. In contrast, this merging experiment did not result in any substantial co-localization to the perinuclear zone in MCF-7/MR-HF-MR and MCF-7/MR-HF cells. All analyses of the fluorescent slides were performed by confocal microscopy.

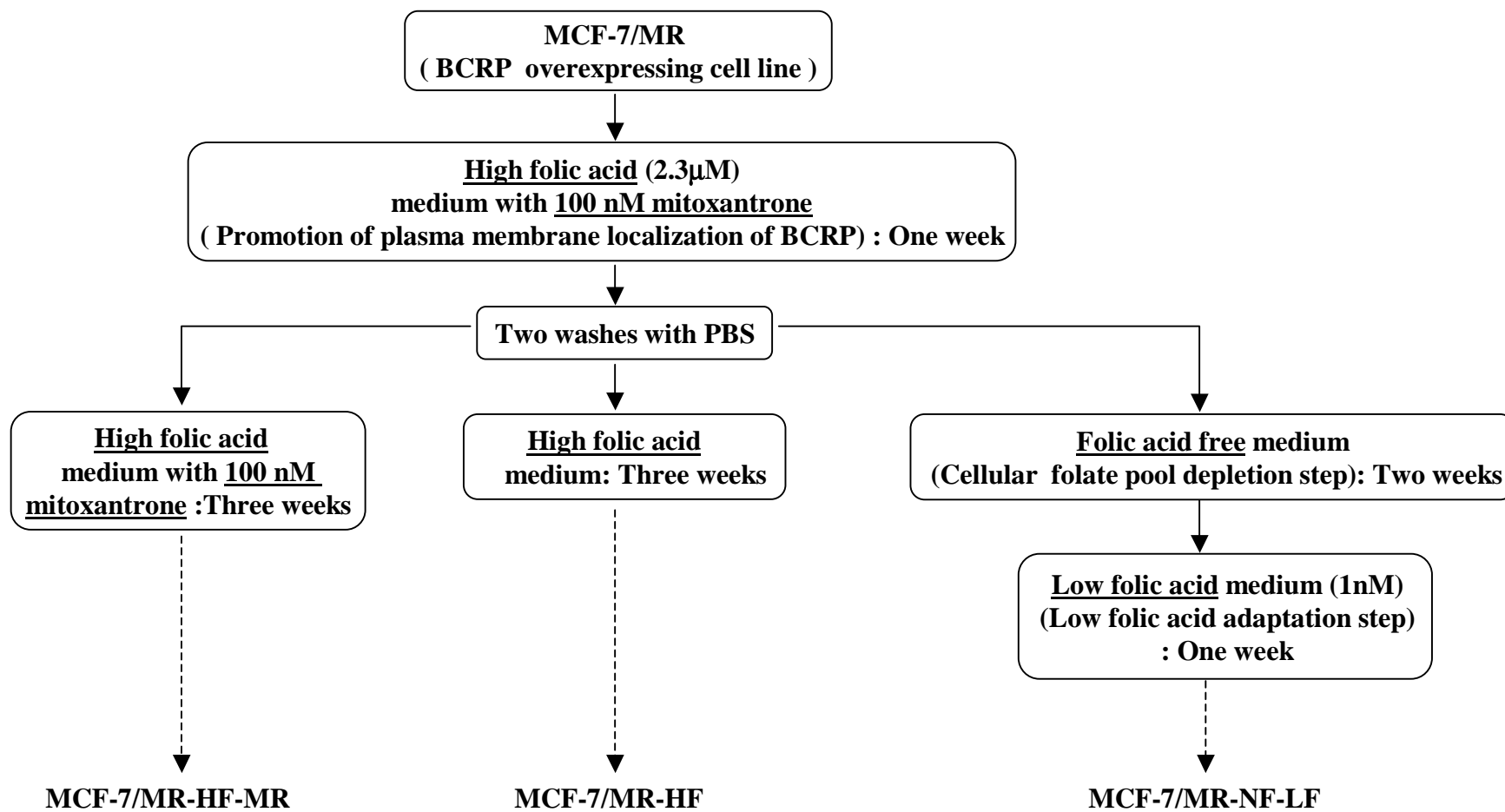
Fig 8: Histogram of rhodamine 123 accumulation in folate-deprived cells and their control counterparts. Monolayer cells growing in 25-mm tissue culture flasks were

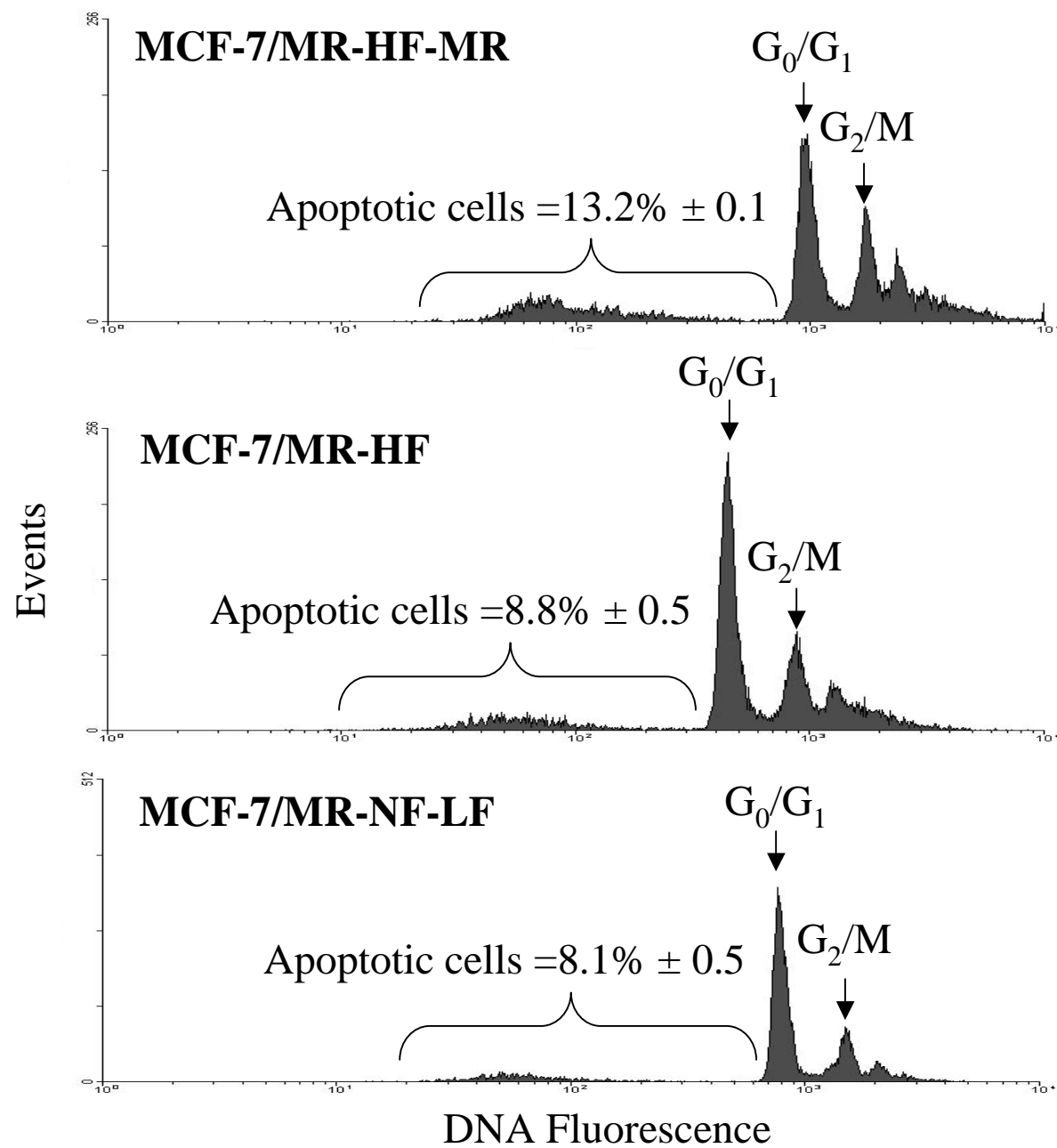
incubated with 750 nM rhodamine123 for 1hr at 37°C. Cells were then washed extensively, lysed and rhodamine 123 was extracted with PBS containing 1% Triton X-100. The fluorescence determined by a fluorescence spectrophotometer was normalized to the relative number of cells present in each culture flask. The *asterisk* denotes that the increased accumulation of rhodamine 123 in folate-deprived cells was statistically significant when compared to parental MCF-7/MR-HF-MR cells ($P=0.017$) or MCF-7/MR-HF cells ($P=0.027$).

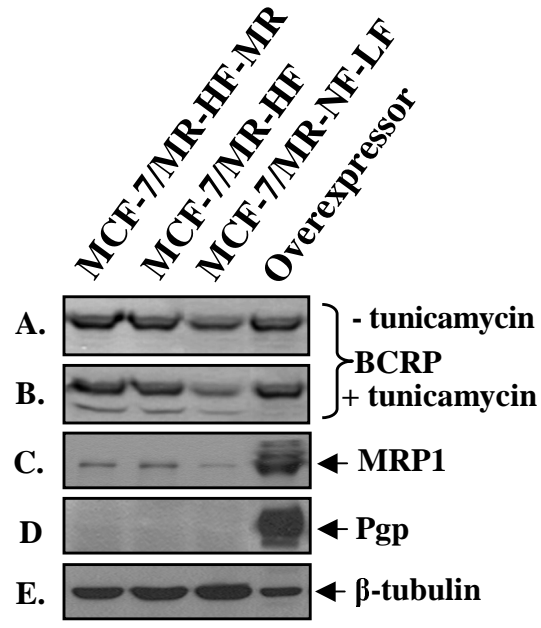
Fig 9: [³H]Folic acid accumulation in parental and short-term folate deprived cells.

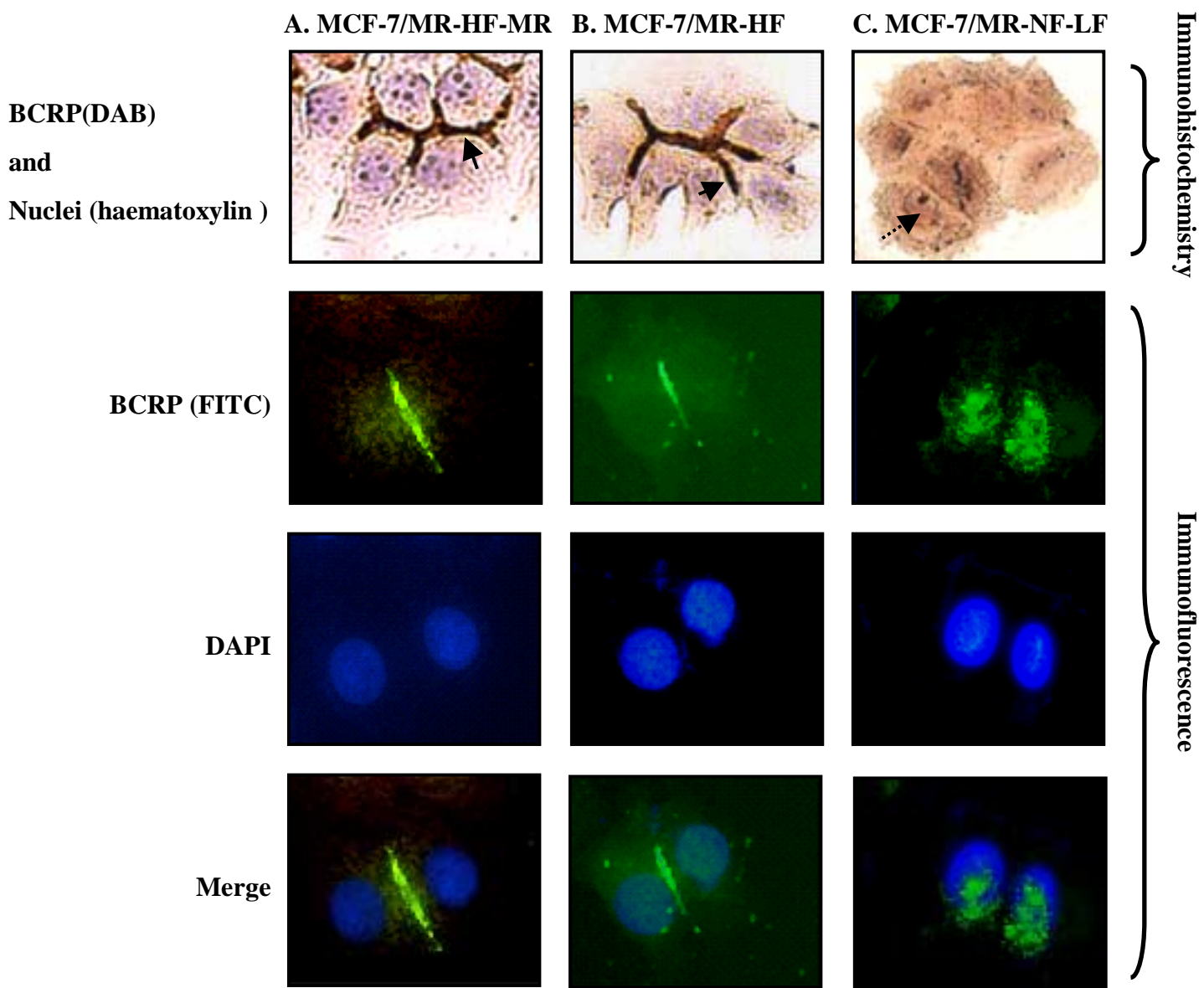
Monolayer cells were washed with folate-free medium and incubated for 30 min at 37°C in HBS containing 2 μ M [³H]folic acid in the presence of 1mM trimetrexate. Transport was stopped by the addition of 10 ml of ice-cold HBS. Then, cells were detached by trypsinization, washed with ice-cold transport buffer, and the final cell pellet was suspended in 0.2 ml water and the radioactivity released was determined using a liquid scintillation spectrometer. The asterisk denotes statistically significant change in the MCF-7/MR-NF-LF subline when compared to its parental MCF-7/MR-HF-MR counterpart ($P=0.0026$).

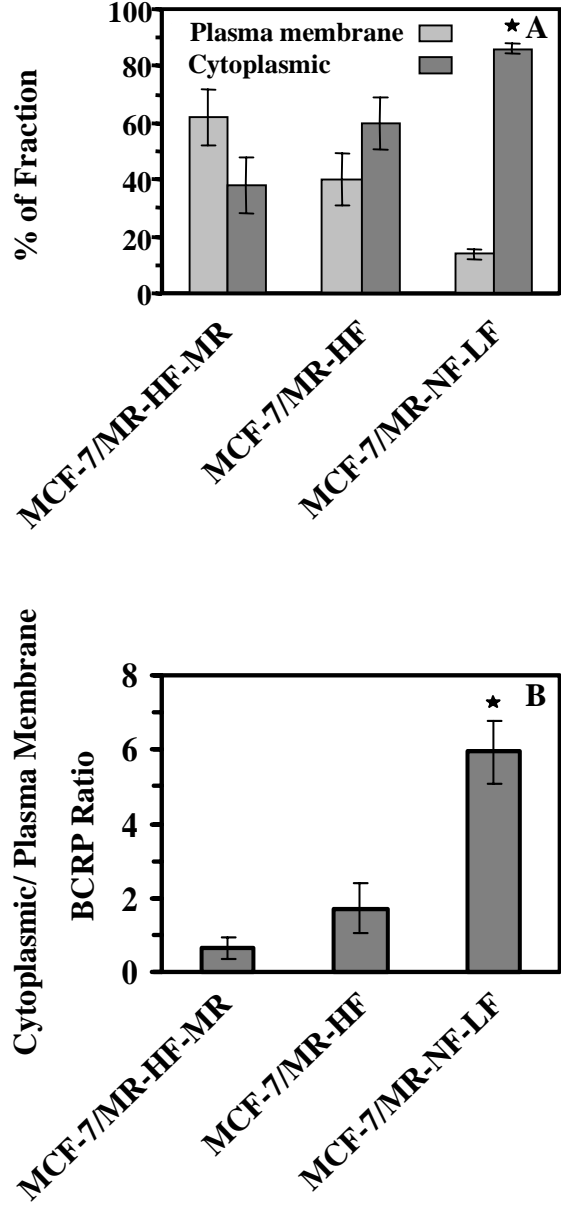
Fig 10: Histogram comparing the association between the percentage of the cytoplasmic BCRP versus the number of cells in the different colonies of folate-deprived cells (C) and their control counterparts (A,B). Note that only in the folate-deprived cells, the percentages of cytoplasmic BCRP were significantly higher in the colonies containing high cell numbers (i.e. cell number per colony > the median cell number of the colonies in the population) than colonies containing low cell numbers (cell number per colony < the median cell number of the colonies) ($P=0.013$).

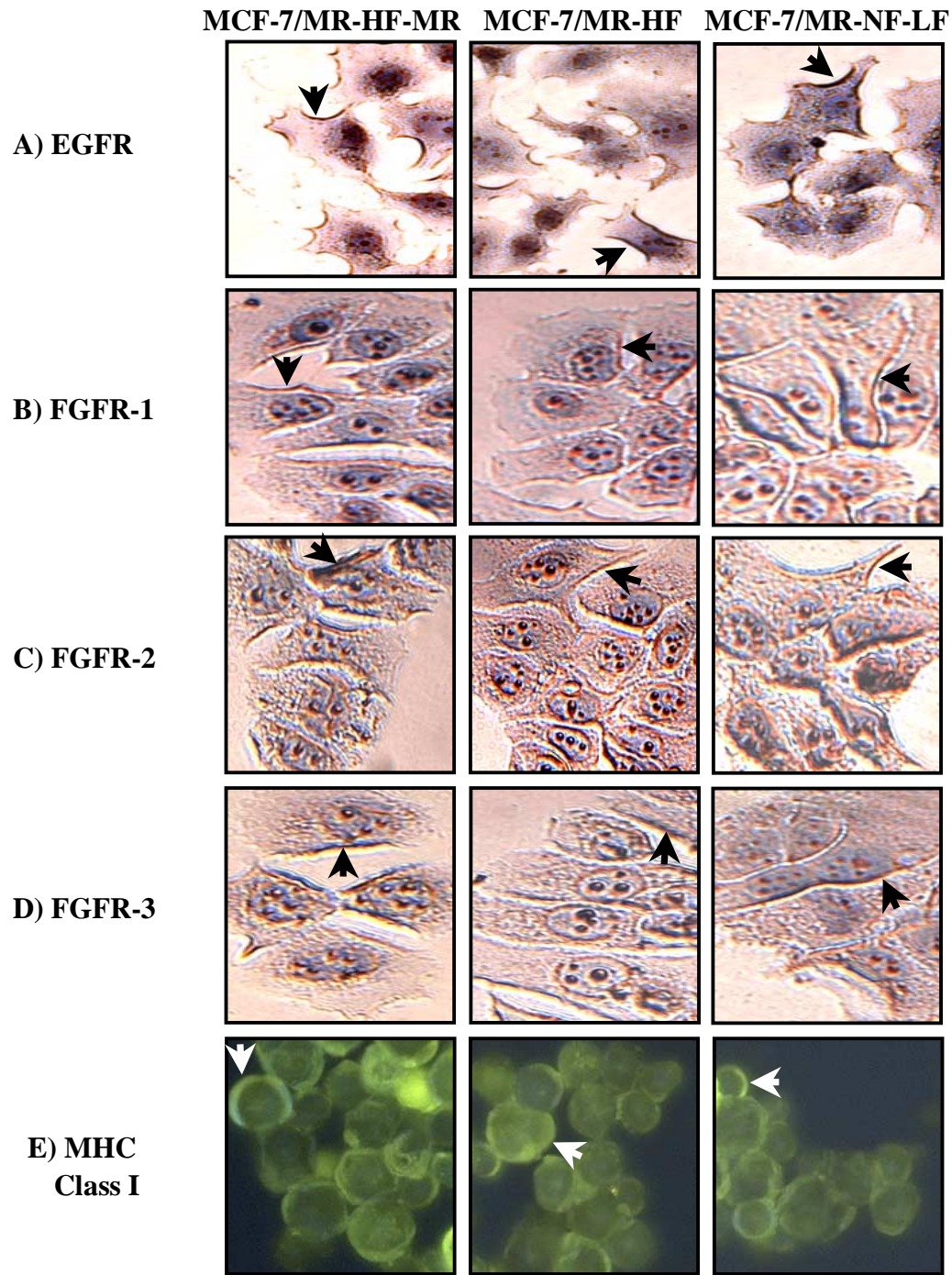


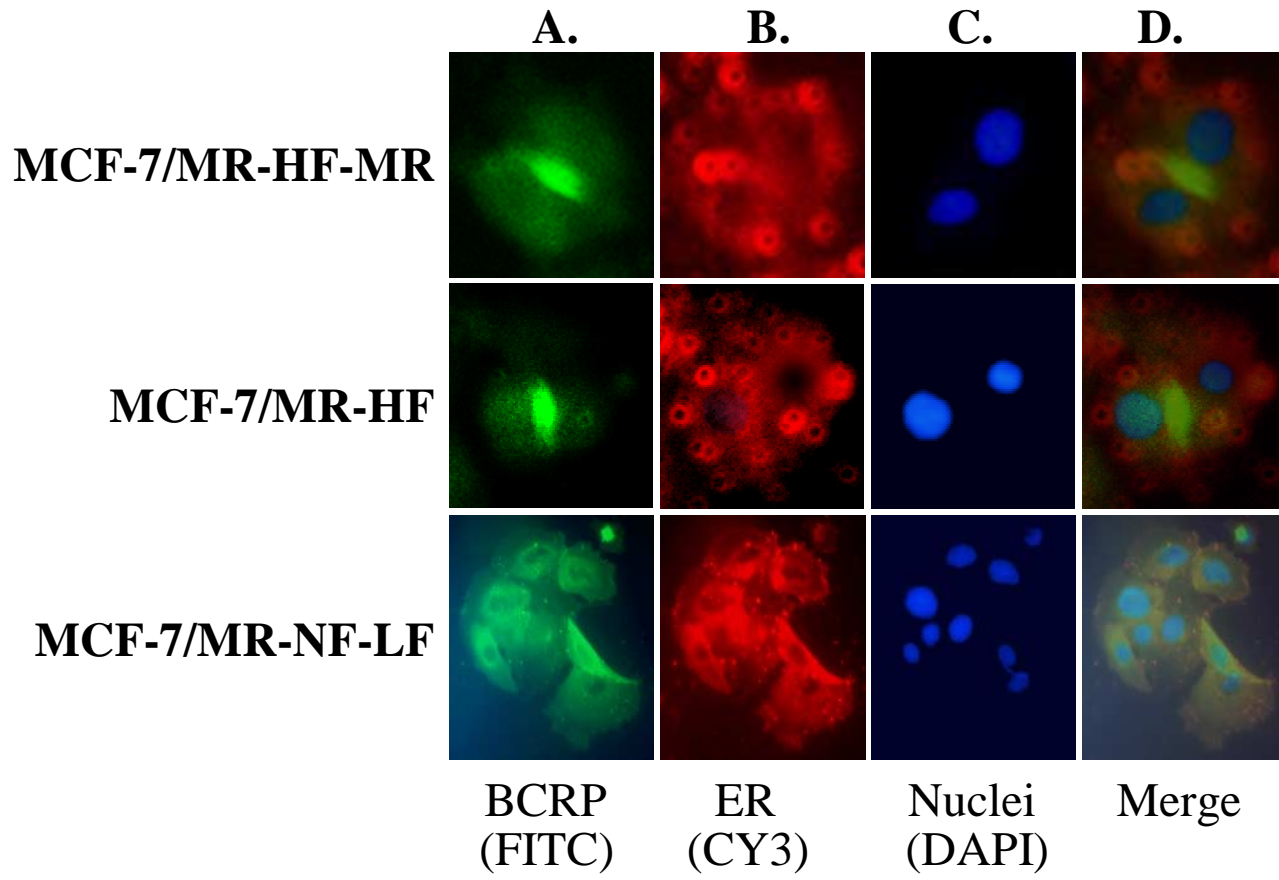












Rhodamine 123 Accumulation

(Arbitrary Units)

